Submitted to
ASCE "Arctic '85"
San Francisco
25-27 Mar '85.

Triaxial Compression Testing of Ice

Gordon F.N. Cox[1] and Jacqueline A. Richter-Menge[2]

Abstract

Procedures have been refined for performing constant-strain-rate triaxial tests ($\sigma_1 > \sigma_2 = \sigma_3$) on ice samples. The equipment is designed such that the confining pressure/axial stress ratio (σ_3/σ_1) remains constant. Sample axial displacements are measured inside the cell on the sample and outside the cell between the cell and the loading piston. In addition to reviewing the development of the equipment and testing procedures, data are presented to illustrate the problems of using outside displacement measurements. In general, direct axial displacement measurements on the sample are essential to obtain accurate test strain rates and ice moduli. This is particularly true for brittle ice at low temperatures, high strain rates, and high confining pressures.

Introduction

An understanding of the confined compressive strength of ice is needed to develop constitutive equations and failure criteria for analytical ice-structure interaction models. During the past several years, a variety of testing techniques have been used to study the behavior of ice under a complex state of stress. The plane-strain compressive strength of freshwater columnar and granular ice was first examined by Frederking (4). Later Timco and Frederking (11), Blanchet and Hamza (1), and Sinha (10) used the same technique to determine the confined compressive strength of sea ice samples. In this type of test, prismatic samples are laterally confined in one direction while they are axially loaded ($\sigma_1 \neq \sigma_2 \neq \sigma_3$, ε_2 or $\varepsilon_3 = 0$). Conventional triaxial tests ($\sigma_1 > \sigma_2 = \sigma_3$ = constant) have been performed by Jones (6) on freshwater granular ice and by Nawwar and others (8) on saline columnar ice. Hausler (5) performed true triaxial tests ($\sigma_1 \neq \sigma_2 \neq \sigma_3$) using a multi-axial loading machine and brush-type loading platens. Most recently, conventional triaxial tests were performed at CRREL on multi-year sea ice (2,3,7). In our tests, the confining pressure was ramped in constant proportion to the axial stress ($\sigma_1 > \sigma_2 = \sigma_3$, σ_3/σ_1 = constant).

In this paper we describe the development of the CRREL triaxial cell. Particular attention is given to the problems we encountered during the development, their effect on the test results, and the measures we took to eliminate the problems. Our experience applies not only to the CRREL triaxial cell but also to other confined and unconfined testing techniques.

[1]Geophysicist, U.S. Army Cold Regions Research and Engineering Laboratory (CRREL), 72 Lyme Road, Hanover, NH, 03755
[2]Research Civil Engineer, U.S. Army CRREL

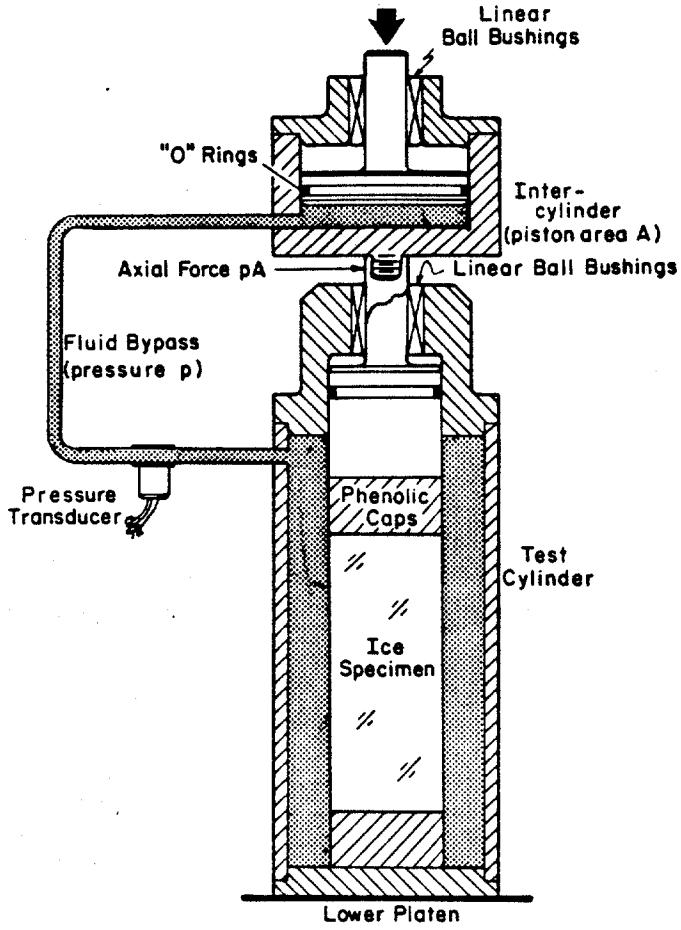

Figure 1. Schematic diagram of triaxial testing equipment.

CRREL Triaxial Cell

The design of the triaxial cell used at CRREL to investigate the mechanical properties of multi-year sea ice was suggested by Mellor (7). Unlike standard triaxial cells, the confining pressure in the CRREL cell is not maintained at a constant level; instead it is ramped in constant proportion to the applied axial stress. This is accomplished by the use of a special intercylinder mounted in the loading train on top of the cell (Fig. 1). For a right cylindrical specimen, the ratio of the confining pressure to the axial stress is determined by the ratio of the diameter of the piston entering the cell (sample diameter) to the diameter of the piston in the upper intercylinder. The ratio is changed by inserting a reducing sleeve and new piston into the upper cylinder. To ensure that the proper σ_3/σ_1 ratio is obtained throughout each test, the fluid pressure is continuously monitored by a pressure transducer.

During the development of the triaxial cell, different techniques were used to measure the sample strain and control the test strain rate. Two types of sample end caps were investigated. Modifications

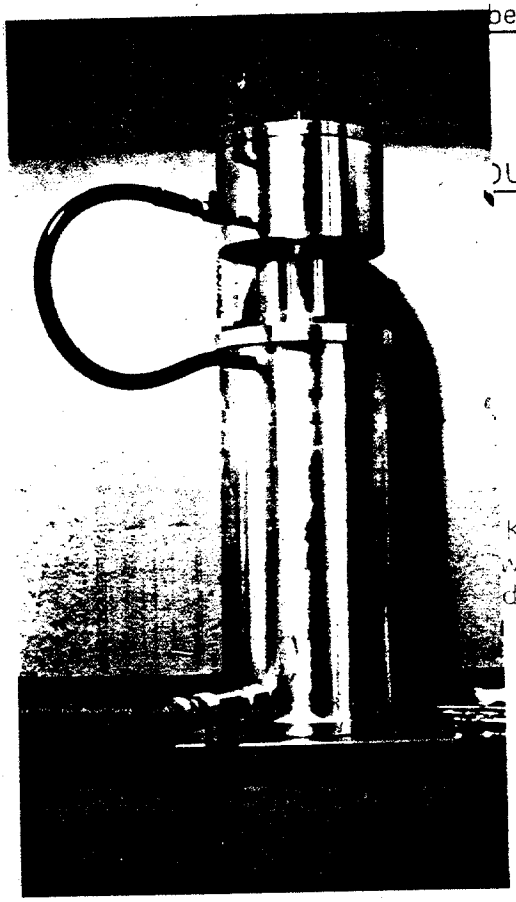

Figure 2. Mark I triaxial cell.

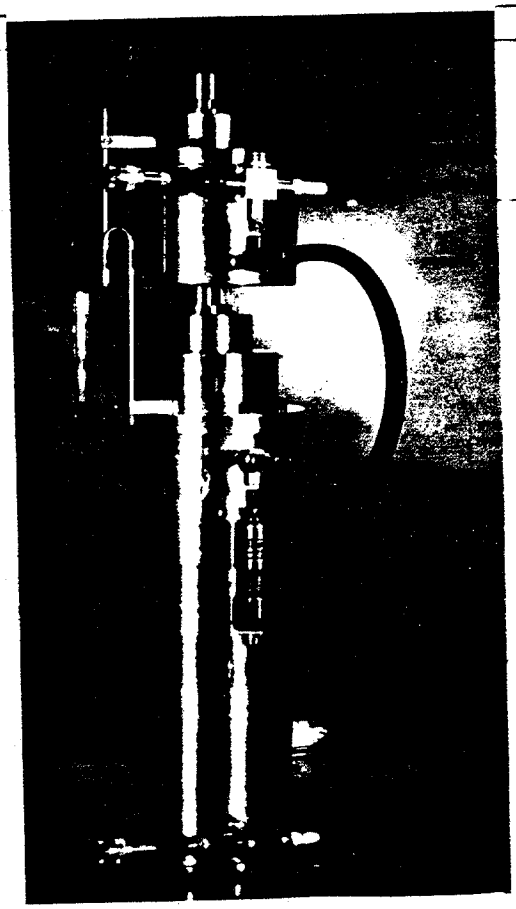

Figure 3. Mark II triaxial cell. Axial displacements were measured with an extensometer which was attached to U-shaped rods mounted on the upper cylinder and top of the cell.

were also made to the cell to increase its capacity. The different versions of the CRREL triaxial cell are discussed below.

Mark I Version

Our Mark I cell is shown in Figure 2. It is similar in design to the triaxial cell shown in Figure 1, with the exception that linear ball bushings were not used to guide the pistons. The sample strain was measured and controlled with an extensometer mounted on U-shaped bars which were attached to the upper cylinder and cell as shown on the Mark II version in Figure 3. It was assumed that the loading train and sample end caps were rigid.

Initial tests at low strain rates and low confining pressures proved to be satisfactory; however, at higher strain rates and σ_3/σ_1, ratios, the aluminum pistons tended to rack slightly and bind. This caused a noticeable variation in the σ_3/σ_1 stress ratio and required that the tests be rejected. Higher than anticipated confined strengths were also measured and the cell capacity was exceeded. It was clear

that the cell would have to be modified before we could proceed with our test program.

Mark II Version

The Mark II triaxial cell is shown in Figures 1 and 3. This version was used to conduct the majority of the tests in the Mechanical Properties of Multi-Year Sea Ice Program (2,3). Linear ball bushings were included in the Mark II version to eliminate the racking and binding problems. The capacity of the cell was also increased by using hardened stainless steel shafts for the piston rods and by increasing the thickness of the end plates on the cell and the size of the end plate bolts.

Later in our test program the method for measuring the axial displacements was improved. In the new setup the strain rate was controlled with the average output from two extensometers. The mounting position of the extensometers was also changed from the upper cylinder to the shaft going into the triaxial cell (Fig. 4). Some test results indicated that the upper cylinder rotated slightly at the beginning of a test. The cell capacity was again increased by increasing the diameter of the stainless steel piston rods.

In general, it is good practice to measure as little of the loading train deformation as possible when transducers cannot be placed directly on the ice. Two transducers, mounted on opposite sides of the sample,

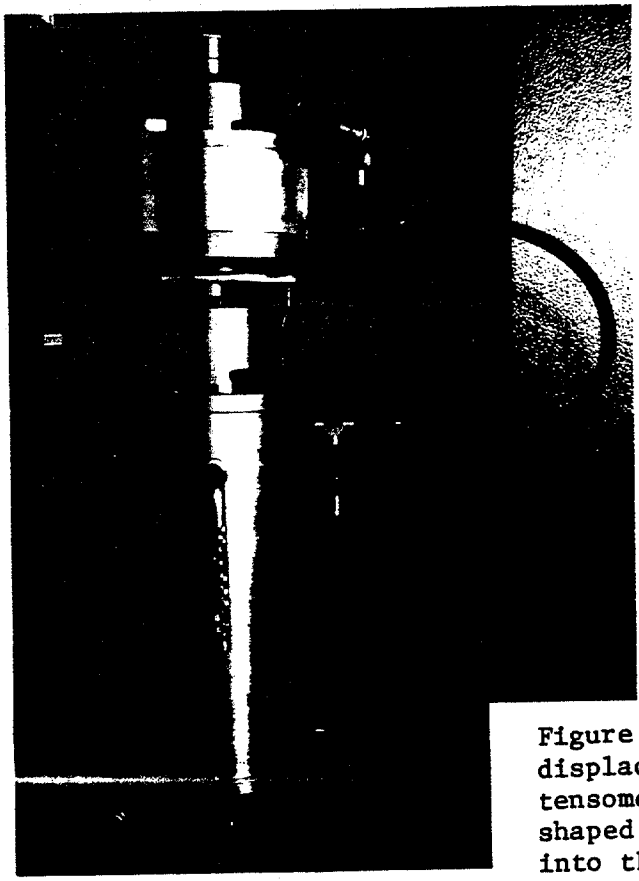

Figure 4. Mark II triaxial cell. Axial displacements were measured with two extensometers which were attached to U-shaped rods mounted on the shaft going into the cell and the top of the cell.

are also desirable, as they provide a measure of the average axial sample displacement.

It appeared that we had solved our testing problems. After these modifications were made, no obvious difficulties were encountered. However, during the analysis of the triaxial test data, we found that the confined initial tangent modulus data were consistently lower than the initial tangent modulus of the uniaxial or unconfined specimens. This caused some concern because, intuitively, we would expect the confined modulus to be greater. Any confinement should reduce the axial displacement for a given load and thereby increase the measured modulus.

After checking our testing techniques and data reduction procedures, it was concluded that the lower confined modulus values were due to the use of the synthane end caps on our samples in the triaxial cell with externally mounted displacement transducers. In effect, because sample displacement were measured outside the triaxial cell, the synthane end caps became a compliant element in an otherwise stiff loading system. If displacements were measured on the sample as in our uniaxial tests, the synthane end caps would not have presented any problem (7).

In addition to providing low confined modulus values, the synthane end caps and externally mounted displacement transducers also resulted in slightly lower ice strain rates.

Despite the problems of using synthane end caps in the triaxial cell, it was hoped that the true ice modulus and strain rate could be determined, given the mechanical properties of the synthane. Uniaxial and triaxial tests were performed on a synthane specimen to determine the synthane properties, and equations were derived to calculate the actual ice modulus, strains and strain rates from the test results.

Synthane Property Tests

Uniaxial and triaxial compression tests were performed on a 4.2-in. (10.6-cm)-dia., 14-in.-(35.6-cm)-long synthane sample at +20° and -10°C. The tests were conducted at two strain rates, 10^{-3} and 10^{-5} s^{-1}. Confining pressure - axial stress ratios of 0, 0.25, and 0.50 were used in the triaxial tests.

From the uniaxial and triaxial tests the synthane was found to have a modulus of 7.77×10^5 lbf/in.^{2} (5.36 GPa) and a Poisson's ratio of 0.21. The modulus and Poisson's ratio varied little with either strain rate or temperature. The tests also provided a measure of the loading train deflection and cell elongation, 1.4×10^{-7} in./lbf (8.0×10^{-10} m/N), which showed little variation with strain rate, confining pressure, or temperature.

Correction for Synthane End Caps

Given the synthane properties and loading train deflection, it is possible to calculate the actual test strain rate and ice modulus. The total measured displacement, $\Delta \ell_t$, is equal to the sum of the

displacements from the ice sample, $\Delta\ell_s$; the synthane end caps, $\Delta\ell_c$; and the loading train and cell walls, $\Delta\ell_\ell$:

$$\Delta\ell_t = \Delta\ell_s + \Delta\ell_c + \Delta\ell_\ell \tag{1}$$

or

$$\frac{\Delta\ell_t}{F} = \frac{\Delta\ell_s}{F} + \frac{\Delta\ell_c}{F} + \frac{\Delta\ell_\ell}{F} \tag{2}$$

where F is the applied load. From the synthane property tests, we have for the load train

$$\frac{\Delta\ell_\ell}{F} = C \tag{3}$$

where C is a constant, and for the two end caps

$$\frac{\Delta\ell_c}{F} = \frac{2\,\ell_c}{A_c E_c}(1-2\,\upsilon_c k) \tag{4}$$

where

ℓ_c = end cap thickness
A_c = end cap area
E_c = end cap modulus
υ_c = end cap Poisson's ratio
k = confining pressure/axial stress ratio

By combining Equations (1), (3) and (4) and dividing by ℓ_s, the sample length, we obtain

$$\frac{\Delta\ell_t}{\ell_s} = \frac{\Delta\ell_s}{\ell_s} + \frac{2\,\ell_c F}{\ell_s A_c E_c}(1-2\,\upsilon_c k) + \frac{CF}{\ell_s} \tag{5}$$

where $\Delta\ell_t/\ell_s$ is the nominal strain, ε_n, and $\Delta\ell_s/\ell_s$ is the true sample strain, ε_s. Solving for the true sample strain in terms of the nominal strain, we get

$$\varepsilon_s = \varepsilon_n - \frac{2\ell_c F}{\ell_s A_c E_c}(1-2\,\upsilon_c k) - C\frac{F}{\ell_s} \tag{6}$$

and by dividing by time, Δt

$$\dot{\varepsilon}_s = \dot{\varepsilon}_n - \frac{2\ell_c \dot{F}}{\ell_s A_c E_c}(1-2\,\upsilon_c k) - C\frac{\dot{F}}{\ell_s} \quad . \tag{7}$$

From Equation (6) we can also obtain a relationship between the measured (E_m) and actual (E_s) confined ice modulus by multiplying by A_s/F, where A_s is the cross-sectional area of the sample:

$$\frac{\varepsilon_s A_s}{F} = \frac{\varepsilon_n A_s}{F} - \frac{A_s}{\ell_s}\left(\frac{2\,\ell_c}{A_c E_c}(1-2\,\upsilon_c k) + C\right)$$

or

$$\frac{1}{E_s} = \frac{1}{E_m} - \frac{A_s}{\ell_s}\left(\frac{2\,\ell_c}{A_c E_c}(1-2\,\upsilon_c k) + C\right) \qquad (8)$$

The actual sample strain rate during a test can be found from Equation (7). At the beginning of the test, $\dot{F}$ is at its maximum and the actual strain rate is at its lowest value for the entire test:

$$\dot{F} = \dot{F}_o = A_s E_m \dot{\varepsilon}_n$$

At the peak stress

$$\dot{F} = \dot{F}_p = 0$$

and

$$\dot{\varepsilon}_s = \dot{\varepsilon}_n \quad .$$

The average strain rate up to the peak stress can be found by using

$$\dot{F}_{avg} = \frac{\sigma_m A_s}{t_m}$$

where σ_m is the peak stress and t_m is the time to failure.

The actual initial modulus, E_s, can be directly determined from Equation (8). Equation (6) can be used to correct sample failure strains.

The measured modulus, strength, and time to failure from several triaxial tests were used to calculate actual strain rates and moduli (3). The calculations indicated that the use of synthane end caps in the triaxial cell had only a slight effect on the actual strain rate during a test. The greatest difference between the nominal (external) and actual strain rates was found to occur under conditions where the ice was the stiffest, that is, at high strain rates, low temperatures, and large σ_3/σ_1, stress ratios. Under these conditions, actual and nominal strain-rates differed by 25%. As significant changes in ice mechanical properties occur over orders of magnitude of change in strain rate, the use of synthane end caps resulted in an undesirable but not serious problem. For a while, aluminum end caps were used on our samples to minimize the end cap deformation problem.

Unfortunately, even with aluminum end caps, the corrected modulus values still appeared to be too low when they were compared to the modulus values obtained from the uniaxial test specimens. This suggested that there were other displacement errors not properly accounted for, such as closure across the end cap/loading piston interface. Recently, Richter-Menge demonstrated that closure errors less than 0.002 in. (5.0×10^{-5} m) can significantly reduce the initial tangent modulus at the beginning of the test when displacement transducers are not placed directly on the ice or the sample end caps (9).

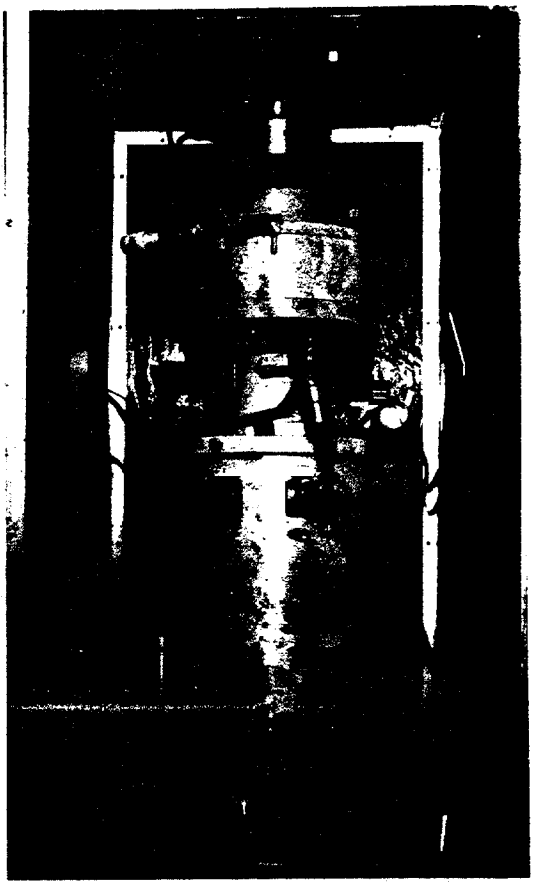

Figure 5. Mark III triaxial cell. Axial displacements were measured between the sample end caps inside the cell. External extensometers were also used to evaluate previous measurement techniques.

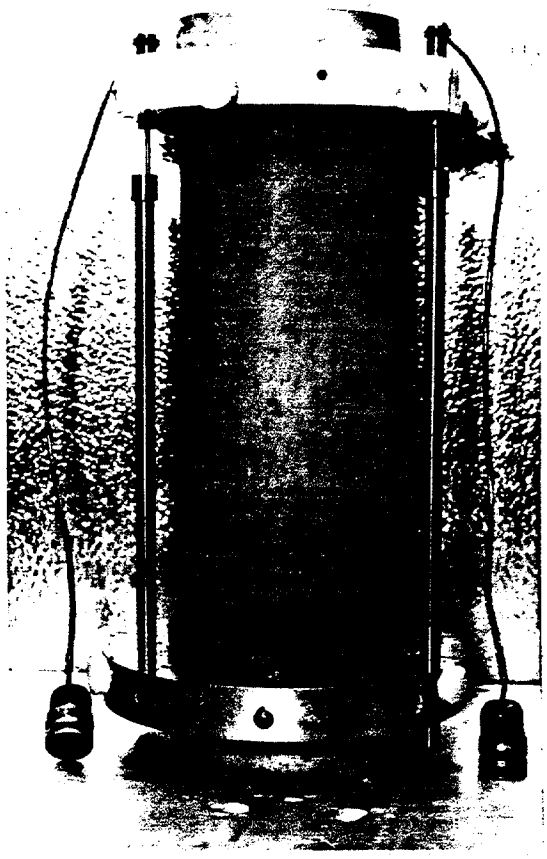

Figure 6. Instrumented triaxial test specimen covered with latex membrane.

Mark III Version

In order to obtain accurate sample strains and ice moduli, we finally enlarged the triaxial cell (Fig. 5) to accommodate an ice sample instrumented with a pair of linear variable differential transducers (LVDTs). The LVDTs are immersible and are capable of withstanding high hydraulic pressures. As we were interested in examining the post-yield behavior of the ice and mechanical properties at large strains, the LVDTs were mounted on the sample end caps (Fig. 6). Earlier work has shown that transducers mounted directly on the ice only provide reliable measurements up to the ice yield strength (7). The LVDTs were used to control the ice strain rate and to measure sample strains and the initial tangent modulus.

A number of tests were performed on our synthane test specimen and on first-year, oriented sea ice samples to evaluate the new cell and LVDTs. The synthane test specimen was used to determine the deformation characteristics of the cell. Measurements of the cell's loading train

deflection and the axial deformation of the cell wall were obtained for given loads and confining pressures. Unlike the previous triaxial cell, axial deformation of the cell wall was significant because of the larger annulus between the sample and cell wall. Tests were also performed on sea ice specimens to compare external extensometer and internal LVDT measurements. We were interested in evaluating our formulas that were used to correct extensometer readings for deformation of the end caps, loading train, and cell wall.

Stress-strain curves for two tests are shown in Figures 7 and 8. The test results in Figure 7 were obtained by controlling the sample strain rate with the LVDTs mounted on the sample end caps. By measuring sample strains inside the cell on the sample, accurate strain rates, strains, and moduli are obtained. The output from the external extensometers is also shown for comparison. In Figure 8 the tests results were obtained by controlling the strain rate with the external extensometers as in the Mark II version triaxial tests. Also shown is the actual stress-strain behavior experienced by the sample as measured by the LVDTs. Equations 6, 7 and 8 were used to correct the extensometer readings considering the deformation of the loading train, cell wall, and sample end caps. The corrected values are compared to the actual readings in Table 1. These results clearly demonstrate that the external extensometer measurements can be corrected and used to

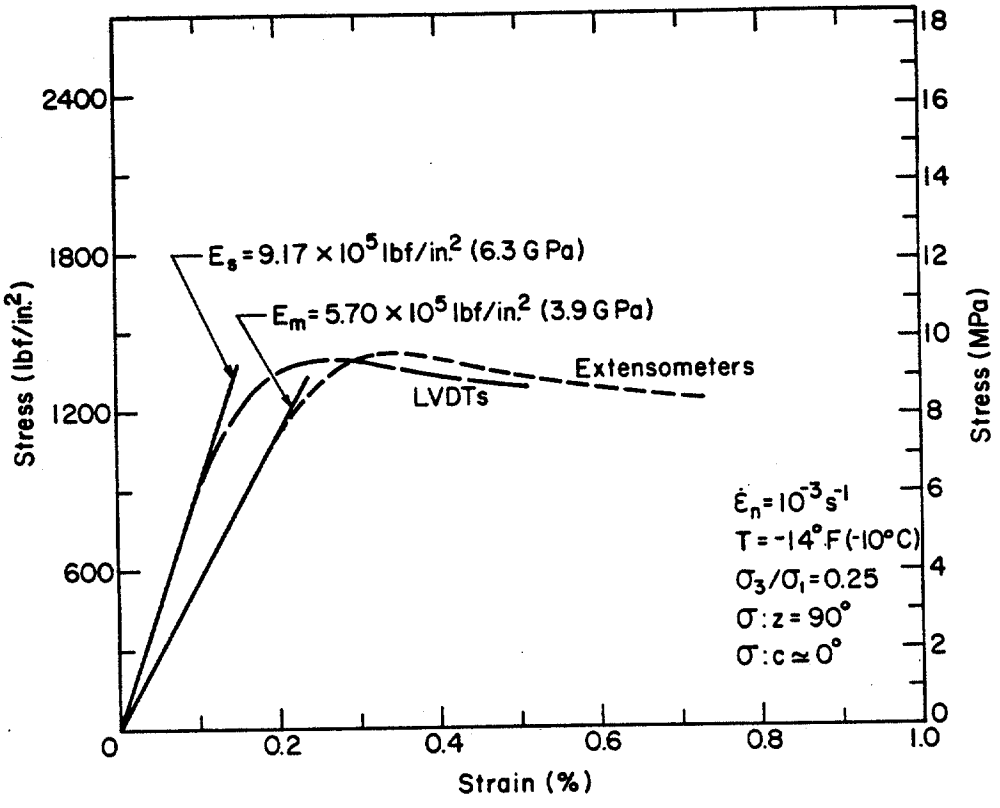

Figure 7. Stress-strain curves for a first-year sea ice sample whose strain rate was controlled by LVDTs mounted on the sample end caps inside the cell. Test results are for an aligned, horizontal (σ:z = 90°) sample loaded parallel to the c-axis (σ:c = 0°).

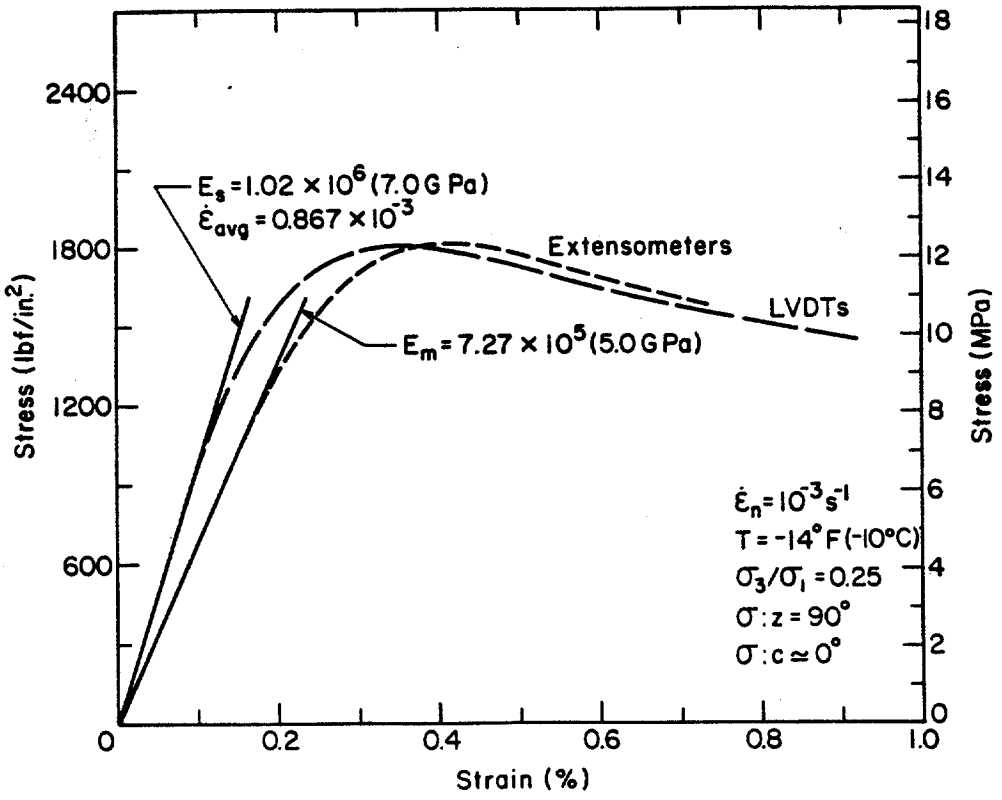

Figure 8. Stress-strain curves for a first-year sea ice sample whose strain rate was controlled by two external extensometers.

Table 1. Comparison between extensometer, corrected extensometer, and actual LVDT measurements for the first-year sea ice sample results shown in Figure 8. ε_f is the sample failure strain.

	Extensometers	Corrected extensometers	Actual LVDTs
$\dot{\varepsilon}_o$, s^{-1}	1×10^{-3}	7.27×10^{-4}	7.95×10^{-4}
$\dot{\varepsilon}_{avg}$, s^{-1}	1×10^{-3}	8.63×10^{-4}	8.67×10^{-4}
ε_f, %	0.413	0.362	0.363
E, lbf/in.^{2}	7.27×10^5	9.14×10^5	1.01×10^6
E, GPa	5.01	6.30	6.97

calculate actual sample strains and strain rates if the cell deformation characteristics are known. However, due to some closure at the loading piston-end cap interface at the beginning of the test, the corrected initial tangent modulus value is still too low. Excellent agreement is obtained for the sample failure strain and average strain rate because the sample displacement at yield is very large compared to the loading piston-end cap closure.

Conclusions

Procedures have been developed for performing "true" constant-strain-rate triaxial tests on ice samples. During the development numerous problems were encountered, and it was necessary to increase the cell capacity and find better ways to measure sample strains.

Analyses of our early triaxial modulus data indicated that our sample strains, as determined by an external extensometer, were in error. In addition to measuring the axial deformation of the sample, we were measuring the deformation of the synthane end caps on the sample, the loading train, and the cell wall. While these deformations were small, they resulted in low confined modulus values and slightly lower ice strain rates.

Equations were then derived to correct the extensometer readings and evaluate the seriousness of the problem. Triaxial tests were also performed on a synthane test specimen to determine the mechanical properties of the synthane and deformation characteristics of the loading cell. The results indicated that actual ice strain rates were up to 25% lower than the nominal strain rate. The greatest difference between the actual and nominal strain rates was found under test conditions where the ice was stiffest; that is, at high strain rate, low temperature, and high confining pressure.

Corrected confined modulus data were still to low. It was determined that initial strain and modulus measurements were also affected by closure at the loading piston-end cap interface. Closures less than 0.002 in. (5.0×10^{-5} m) were sufficient to reduce measured moduli by 50%. While it was possible to correct the test data and determine the average strain rate and failure strain for a given test, transducers in the cell were required to measure reliable modulus data.

The triaxial cell was enlarged and LVDTs mounted on the sample end caps were used to control the test strain rate and measure sample strains. Additional testing proved that the equations developed to correct the earlier strain and strain rate data were valid and that transducers on the sample were only needed for accurate moduli data.

In light of our experience, we strongly recommend that displacement transducers be placed on the sample, regardless of the type of test. Only by having transducers mounted on the ice are we assured of the actual test strain, strain rates, and moduli. As most portable field testing machines are relatively compliant, it is even more important to measure displacements on the sample in the field.

Acknowledgements

This study was sponsored by Shell Development Company and the Minerals Management Service of the U.S. Department of the Interior, with support from Amoco Production Company, Exxon Production Research Company, and Sohio Petroleum Company.

Appendix. - References

1. Blanchet, D. and Hamza, H. "Plane-strain compressive strength of first-year Beaufort Sea ice", Proceedings of the Seventh International Conference on Port and Ocean Engineering under Arctic Conditions, Helsinki, Finland, vol. 3, pp. 84-96, 1983.

2. Cox, G.F.N., Richter-Menge, J.A., Weeks, W.F., Mellor, M. and Bosworth, H. "Mechanical properties of multi-year sea ice, Phase I: Test results," U.S. Army Cold Regions Research and Engineering Laboratory, Report 84-9, 105 p., 1984.

3. Cox, G.F.N., Richter-Menge, J.A., Weeks, W.F., Mellor, M., Bosworth, H., Durell, G. and Perron, N. "Mechanical properties of multi-year sea ice, Phase II: Test results," U.S. Army Cold Regions Research and Engineering Laboratory, report in press.

4. Frederking, R. "Plane-strain compressive strength of columnar-grained and granular-snow ice," Journal of Glaciology, vol. 18, no. 80, pp. 505-516, 1977.

5. Hausler, F.U. "Multiaxial compressive strength tests on saline ice with brush-type loading platens," Proceedings of the IAHR International Symposium on Ice, Quebec, Canada, vol. 2, pp. 526-539, 1981.

6. Jones, S.J. "The confined compressive strength of polycrystalline ice," Journal of Glaciology, vol. 28, no. 98, pp. 171-177, 1982.

7. Mellor, M., Cox, G.F.N. and Bosworth, H. "Mechanical properties of multi-year sea ice, Testing techniques," U.S. Army Cold Regions Research and Engineering Laboratory, Report 84-8, 39 p., 1984.

8. Nawwar, A.M., Nadreau, J.P. and Wang, Y.S. "Triaxial compressive strength of saline ice," Proceedings of the Seventh International Conference on Port and Ocean Engineering under Arctic Conditions, Helsinki, Finland, vol. 3, pp. 193-201, 1983.

9. Richter-Menge, J.A. "Static determination of Young's modulus in sea ice," Cold Regions Science and Technology, vol. 9, no. 3, pp. 283-286, 1984.

10. Sinha, N. "Confined strength and deformation of second-year columnar-grained sea ice in Mould Bay," Paper prepared for the Fourth International Symposium on Offshore Mechanics and Arctic Engineering, Dallas, Texas, 1985.

11. Timco, G.W. and Frederking, R. "Confined compressive strength of sea ice," Proceedings of the Seventh International Conference on Port and Ocean Engineering under Arctic Conditions, Helsinki, Finland, vol. 1, pp. 243-253, 1983.

TITLE OF PAPER SHOULD BE ON THIS LINE ON PAGE 1

[illegible] typed text, tables, and figures within blue borders. Material produced at 75% of typed size.